

OXIDATION OF  $ZrB_2-SiC$

*Spelled out in a Title!*

Elizabeth J. Opila  
Cleveland State University  
NASA Glenn Research Center  
21000 Brookpark Rd.  
Cleveland, OH 44135

Michael C. Halbig  
US Army Research Laboratory  
NASA Glenn Research Center  
21000 Brookpark Rd.  
Cleveland, OH 44135

ABSTRACT

In this paper the oxidation behavior of  $ZrB_2-20$  vol% SiC is examined. Samples were exposed in stagnant air in a zirconia furnace (Deltech, Inc.) at temperatures of 1327, 1627, and 1927°C for ten ten-minute cycles. Samples were removed from the furnace after one, five, and ten cycles. Oxidized material was characterized by mass change when possible, x-ray diffraction (XRD), scanning electron microscopy (SEM), and energy dispersive spectroscopy (EDS). Oxidation kinetics, oxide scale development, and matrix recession were monitored as a function of time and temperature. Oxidation and recession rates of  $ZrB_2 - 20$  vol% SiC were adequately modeled by parabolic kinetics. Oxidation rates of this material are rapid, allowing only very short-term application in air or other high oxygen partial pressure environments.

INTRODUCTION

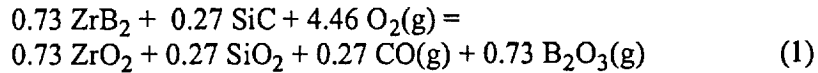
$ZrB_2$  and its resulting oxide,  $ZrO_2$ , have melting points of 3050 and 2710°C, respectively. Because of this high temperature capability, Ultra High Temperature Ceramics (UHTCs), which include Zr- and the related Hf-based borides, nitrides, and carbides, are targeted for use in the temperature range of 1600 to 2000°C where other oxides such as  $SiO_2$  and  $Al_2O_3$  are at or near their melting points. However, it is also known that  $ZrO_2$  is not a highly protective oxide. Solid state transport of oxygen through this material is rapid. Recession rates of  $ZrB_2$  due to oxidation are expected to be rapid in high oxygen partial pressure environments. Lifetimes of components based on  $ZrB_2$  recession rates will therefore be relatively short in highly oxidizing environments.

The oxidation resistance of  $ZrB_2$ -based materials has been previously studied. These materials were first developed in the 1960's [1]. At this time it was found that 20 vol% SiC additions provided the most oxidation resistance by promoting

---

This report is a preprint of an article submitted to a journal for publication. Because of changes that may be made before formal publication, this preprint is made available with the understanding that it will not be cited or reproduced without the permission of the author.

the formation of borosilicate glass. This borosilicate glass afforded more oxidation protection than boria since it is more viscous, has a higher melting temperature and a lower vapor pressure, and is more of a barrier to oxygen diffusion. The formation of both condensed phase and gas phase oxidation products makes determination of recession kinetics by weight change difficult. These phases are shown in the following reaction for ZrB<sub>2</sub> - 20 vol% SiC (27 mol% SiC):



Elegant TGA experiments were devised to distinguish between the weight gain by condensed phase formation and weight loss by formation of volatile species [2]. It was concluded that the boron component of ZrB<sub>2</sub> is generally completely volatilized in high temperature reactions. Finally, this class of materials has received more recent interest as leading edge materials for re-entry vehicles [3] and as high temperature structural materials [4].

At NASA Glenn Research Center, there is interest in determining whether these materials might also find application in the higher oxygen potential environments of short-life space propulsion applications such as specialized turbopumps or satellite propulsion systems. The goal of this work is to understand the oxidation mechanism and develop prediction capability for the recession rate of ZrB<sub>2</sub>-SiC in higher oxygen partial pressure environments.

## EXPERIMENTAL

ZrB<sub>2</sub>-SiC material was obtained from Materials and Machines (Tucson, AZ). Sample coupons were 2.54 x 1.27 x 0.32 cm. Coupons were ultrasonically cleaned in detergent, de-ionized water, acetone and alcohol prior to exposure. Initial sample weights (to an accuracy of 0.00005g) and dimensions (to an accuracy of 0.001 cm) were recorded. Three samples were loaded into a slotted ZrO<sub>2</sub> refractory brick. Samples were exposed to ten-minute oxidation cycles in stagnant air at 1327°C in a box furnace with molydisilicide heating elements (CM, Inc. Rapid Temp Furnace, Bloomfield NJ). One sample was removed after one cycle, five cycles and ten cycles. A maximum exposure time of 100 minutes was thus achieved. Similar exposures were conducted at 1627 and 1927°C using a bottom-loading furnace with zirconia heating elements (DelTech, Inc., Denver, CO).

Post-test analyses included the following. Weight change was measured, where possible. Some of the samples stuck to the sample holder during oxidation due to extensive glass formation. X-Ray Diffraction (XRD) was used to identify oxide phases present after exposure. After surface microstructural analysis by

Scanning Electron Microscopy (SEM) and Energy Dispersive Spectroscopy (EDS), samples were cross-sectioned and polished to 1 $\mu$ m diamond in nonaqueous polishing media. Water was avoided to preserve any boron that might be present as an oxidation product. The amount of substrate recession was determined from the difference between the initial thickness and the thickness of unreacted material that was measured in low magnification SEM micrographs of sample cross-sections. Thickness measurements obtained from micrographs were corrected based on a NIST magnification reference standard.

## RESULTS

Macrographs of the samples after oxidation are shown in Figure 1. Oxide formation is visible on the samples tested at 1327°C. Extensive glass formation was observed on samples exposed at 1627°C. Samples oxidized at 1927°C formed an orange oxide after 10 minutes that became grayer with time. At this exposure temperature, swelling of the samples occurred in amounts up to 80%. XRD analyses show the surface oxidation product is largely monoclinic ZrO<sub>2</sub> under all conditions. Figure 2 shows macrographs of the sample cross-sections after oxidation. Oxide scales are visible to the eye beginning with exposures at 1627°C. The sample exposed at 1927°C for 10 cycles (100 minutes) is almost completely consumed.

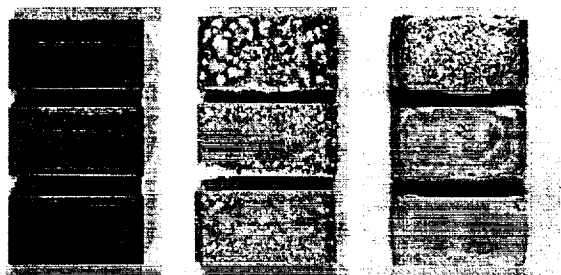


Figure 1. Oxidized ZrB<sub>2</sub>-SiC.  
Left to right: 1327, 1627, 1927°C.  
Bottom to top: 1 cycle, 5 cycles, 10 cycles.



Figure 2. Cross-sections of oxidized samples. Left to right: 1327°C 1 cycle, 10 cycles; 1627°C 1 cycle, 10 cycles; 1927°C 1 cycle, 10 cycles.

SEM and EDS results for sample cross-sections are shown in Figures 3 through 5. SEM and EDS (Hitachi S-4700 Field Emission SEM/EDS) results were obtained at 6kV where sensitivity to boron is high. After exposure at 1327°C for 10 cycles, the oxide scale was about 30  $\mu$ m thick and composed of ZrO<sub>2</sub> with unoxidized SiC particles embedded in the scale as shown in Figure 3. EDS analysis of the ZrO<sub>2</sub> scale in this and all subsequent samples showed some boron

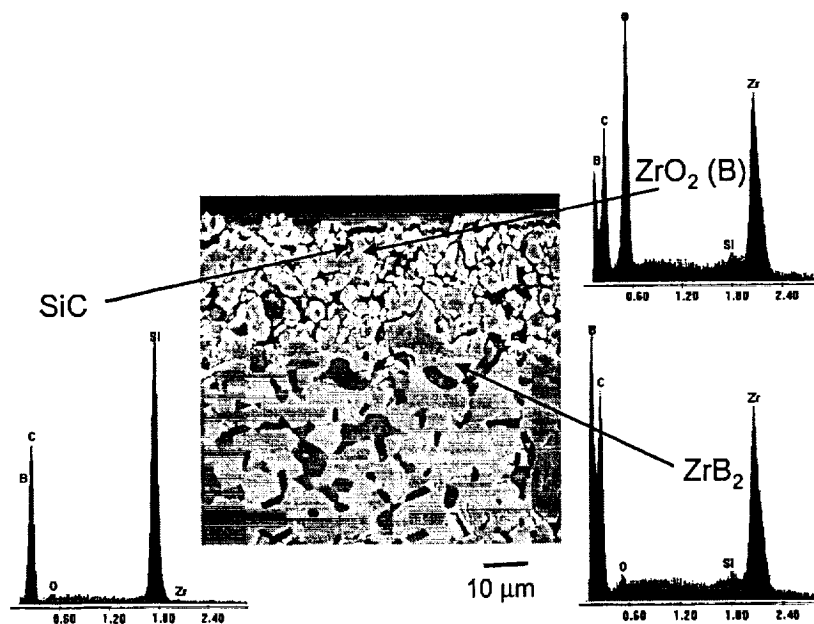


Figure 3. SEM/EDS results for a cross-section of  $ZrB_2$ -SiC oxidized at  $1327^\circ\text{C}$  in air for 10 cycles.

content. Figure 4 shows the sample cross-section after exposure at  $1627^\circ\text{C}$  for 10 cycles as well as the results of an EDS line scan. The oxide scale was about  $150\ \mu\text{m}$  thick. Beginning from the surface, the scale was composed of amorphous  $\text{SiO}_2$  followed by a layer of primarily  $\text{ZrO}_2$  in a continuous silica-rich glassy phase. No boron was detected in the glassy phase. A discrete  $\text{ZrO}_2/\text{ZrB}_2$  boundary was followed by a SiC depleted region of  $\text{ZrB}_2$  of about another  $100\ \mu\text{m}$  thickness. This SiC depletion layer was observed in previous work, both the work at high temperatures and high oxygen partial pressures [1] as well as in exposures at lower temperatures, but only in reduced oxygen partial pressures [2]. This SiC depletion was attributed to active oxidation of the SiC to form  $\text{SiO}(\text{g})$  [2]. Figure 5 shows the sample cross-section after exposure at  $1927^\circ\text{C}$  for 10 cycles. Here, the oxide scale was over 1 mm thick. The scale was composed of  $\text{ZrO}_2$  in a silica-rich glassy phase. No SiC depletion layer was observed.

Figures 6 and 7 show the weight change and substrate recession plotted as a function of the square root of time. Weight change results are shown for two separate tests at  $1327^\circ\text{C}$  showing good repeatability. Weight change results are not available at  $1927^\circ\text{C}$  due to reactions with the sample holder. The straight lines in Figures 6 and 7 indicate parabolic kinetics. The oxidation rate is limited by transport through a growing layer. The slope of each line is equal to the square

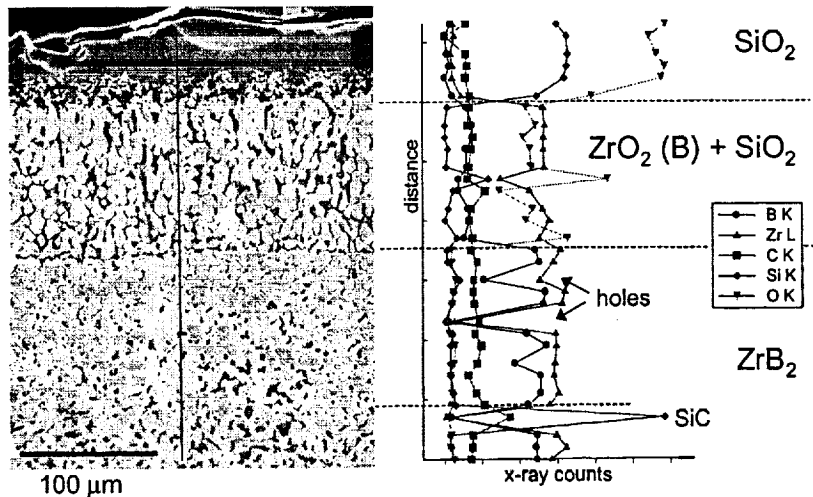


Figure 4. SEM and EDS line scan results for a cross-section of  $ZrB_2$ -SiC oxidized at  $1627^\circ\text{C}$  in air for 10 cycles.

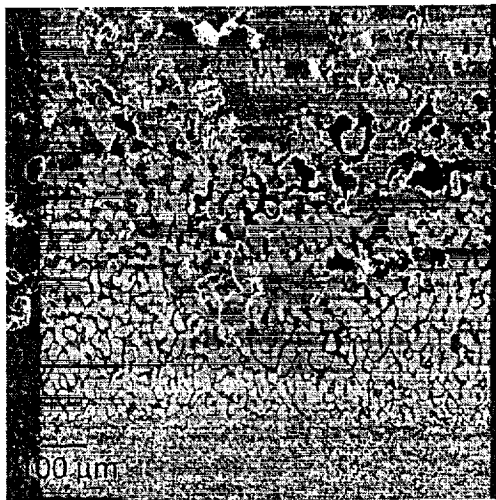


Figure 5. SEM results for a cross-section of  $ZrB_2$ -SiC oxidized at  $1927^\circ\text{C}$  in air for 10 cycles.

root of the parabolic rate constant. Parabolic rate constants are summarized in Table 1. In addition, it should be possible to calculate the parabolic rate constant in terms of weight change,  $k_p$ , from the parabolic rate constant in terms of recession,  $k_p''$ , (and vice versa) if the correct oxidation reaction is known. This has been done using Equation 1 and the following expression.

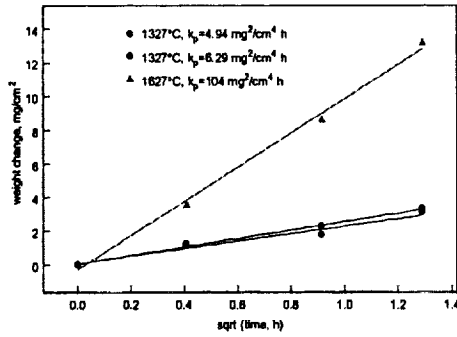


Figure 6. Parabolic weight change kinetics for  $ZrB_2$ -SiC oxidation.

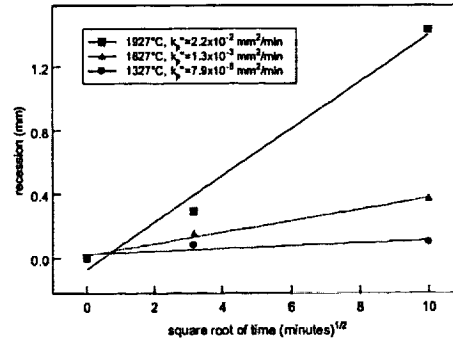


Figure 7. Parabolic recession kinetics for  $ZrB_2$ -SiC oxidation.

**Table 1: Measured and calculated parabolic rate constants for  $ZrB_2$ -SiC oxidation**

	measured recession, $k_p''$ (mm <sup>2</sup> /min)	measured $\Delta wt.$ , $k_p$ (mg <sup>2</sup> /cm <sup>4</sup> h)	calculated $\Delta wt.$ , $k_p$ (mg <sup>2</sup> /cm <sup>4</sup> h)
1327°C	$7.9 \times 10^{-5}$	4.9, 6.3	1.6
1627°C	$1.3 \times 10^{-3}$	$1.0 \times 10^2$	$2.6 \times 10^2$
1927°C	$2.2 \times 10^{-2}$	not available	$4.3 \times 10^3$

$$k_p = k_p'' \rho_{\text{matrix}}^2 \left( \frac{\text{wt. gain / mole}}{\text{wt. matrix consumed / mole}} \right)^2 \quad (2)$$

Here,  $\rho$  is the density of the  $ZrB_2$ -SiC matrix. This equation does not account for the SiC lost in the depletion layer. Nevertheless, the results of measured and calculated  $k_p$  are in good agreement.

Recession rates measured in this work are compared to measured parabolic conversion rates available in the literature [1] in Figure 8. Agreement is poor here, although the studies are in better agreement at 1927°C. It is probable that the parabolic conversion rates do not include the SiC depleted region in the recession measurement, thus accounting for the difference.

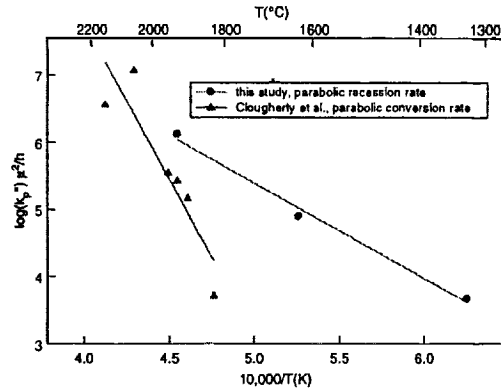


Figure 8. Comparison of oxidation rates of  $ZrB_2$ -SiC to those found in literature.

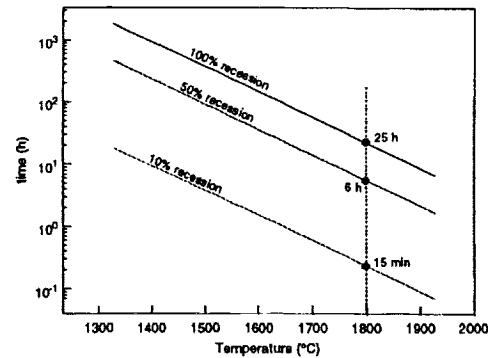


Figure 9. Estimated recession times for  $ZrB_2$ -SiC assuming 0.3 cm thick sample exposed in hot air on one side.

Results of this study allow recession rate predictions as a function of time and temperature. An example is shown in Figure 9. Assuming parabolic oxidation kinetics, for a 0.3 cm thick sample exposed to air on one side at  $1800^\circ\text{C}$ , 10% recession will occur by 15 min., 50% recession by 6h, and 100% consumption by 25h. A time-temperature-recession map such as this can be easily calculated for the desired sample thickness and number of exposed sides using only the recession rate constant.

## DISCUSSION

### Active Oxidation of SiC in Depletion Layer

Active oxidation of SiC below the oxide layer seems the most likely explanation for the depletion observed at  $1627^\circ\text{C}$ . Based on the equilibrium between  $ZrB_2$  and  $ZrO_2$ , a maximum oxygen partial pressure of  $10^{-13}$  atm was calculated at this interface. This seems high enough for appreciable active oxidation of SiC. Continued active oxidation to greater depths might occur by the transport of the available oxygen through the large scale porosity left by the depleted SiC. This remains to be confirmed. As  $SiO(g)$  is transported outward to the surface and a higher oxygen partial pressure is encountered, the  $SiO(g)$  would further oxidize to a condensed phase  $SiO_2$ . The rate of SiC depletion is of importance since the holes left in the  $ZrB_2$  by this process clearly limit the structural capabilities of the material in application.

### Presence of Boron in the Zirconia

Several possible explanations exist for the boron observed in the  $ZrO_2$  by EDS. The first is that boron is present in the zirconia on a substitutional site for the oxygen resulting in a "zirconium oxyboride". A second possibility is that boria is

found in nanoporosity within the zirconia and that the energy of vaporization is overcome by capillary forces. Evidence for retention of boron in the oxide scale has been previously observed, however, analysis to date has not confirmed its chemical state [4,5], i.e. oxide vs. substitutional site. This issue is of practical interest if the boron affects the transport of oxidant in the scale, thereby affecting the recession rate.

## CONCLUSIONS

Oxidation and recession rates of  $ZrB_2$  - 20 vol% SiC are adequately modeled by parabolic kinetics, at least up to times of 100 minutes. From these results, recession rates of this material in air can be predicted between 1327 and 1927°C. Oxidation rates of this material are rapid allowing only very short-term application in air or other high oxygen partial pressure environments. Additional work is required to understand both the SiC depletion layer observed under some conditions as well as the presence of boron in the zirconia layer and the effects of these phenomena on the measured recession rate.

## ACKNOWLEDGMENTS

The authors would like to acknowledge the contributions of Ralph Garlick (NASA Glenn) for the XRD results, Terry McCue (Dynacs/NASA Glenn) for assistance with the FE-SEM, and Nathan Jacobson (NASA Glenn) for helpful discussions regarding active oxidation.

## REFERENCES

1. E.V. Clougherty, R.L. Pober, L. Kaufman, "Synthesis of Oxidation Resistant Metal Diboride Composites," *Trans. Met. Soc. AIME*, 242, 1077-1082 (1968).
2. W.C. Tripp, H.H. Davis, H.C. Graham, "Effect of an SiC Addition on the Oxidation of  $ZrB_2$ ," *Cer. Bull.* 52 [8] 612-616 (1973).
3. J.D. Bull, D.J. Rasky, C.C. Karika, "Stability Characterization of Diboride Composites under High Velocity Atmospheric Flight Conditions," pp. T1092-T1106 in 24<sup>th</sup> International SAMPE Technical Conference, October 20-22, 1992.
4. Opeka, M.M., Talmy, I.G., Wuchina, E.J., Zaykoski, J.A., Causey, S.J., "Mechanical, Thermal, and Oxidation Properties of Refractory Hafnium and Zirconium Compounds," *J. Eur. Cer. Soc.* 19, 2405-2414 (1999).
5. A. Metcalfe, N. Elsner, D. Allan, E. Wuchina, M. Opeka, E. Opila, "Oxidation of Hafnium Diboride," pp. 489-501 in High Temperature Corrosion and Materials Chemistry, eds. M. McNallan, E. Opila, T. Maruyama, T. Narita, The Electrochemical Society, Pennington, NJ, 2000.